Review of Scientific Instruments

Understanding and eliminating artifact signals from diffusely scattered pump beam in measurements of rough samples by time-domain thermoreflectance (TDTR)

Cite as: Rev. Sci. Instrum. **87**, 064901 (2016); https://doi.org/10.1063/1.4952579
Submitted: 23 February 2016 • Accepted: 12 May 2016 • Published Online: 03 June 2016

Bo Sun and Yee Kan Koh

REVIEW OF SCIENTIFIC INSTRUMENTS **87**, 064901 (2016)

Understanding and eliminating artifact signals from diffusely scattered pump beam in measurements of rough samples by time-domain thermoreflectance (TDTR)

Bo Sun[1] and Yee Kan Koh[1,2,a)]
[1]*Department of Mechanical Engineering, National University of Singapore, 9 Engineering Drive 1, Singapore 117576*
[2]*Centre of Advanced 2D Materials, National University of Singapore, Singapore 117542*

(Received 23 February 2016; accepted 12 May 2016; published online 3 June 2016)

Time-domain thermoreflectance (TDTR) is a pump-probe technique frequently applied to measure the thermal transport properties of bulk materials, nanostructures, and interfaces. One of the limitations of TDTR is that it can only be employed to samples with a fairly smooth surface. For rough samples, artifact signals are collected when the pump beam in TDTR measurements is diffusely scattered by the rough surface into the photodetector, rendering the TDTR measurements invalid. In this paper, we systemically studied the factors affecting the artifact signals due to the pump beam leaked into the photodetector and thus established the origin of the artifact signals. We find that signals from the leaked pump beam are modulated by the probe beam due to the phase rotation induced in the photodetector by the illumination of the probe beam. As a result of the modulation, artifact signals due to the leaked pump beam are registered in TDTR measurements as the out-of-phase signals. We then developed a simple approach to eliminate the artifact signals due to the leaked pump beam. We verify our leak-pump correction approach by measuring the thermal conductivity of a rough InN sample, when the signals from the leaked pump beam are significant. We also discuss the advantages of our new method over the two-tint approach and its limitations. Our new approach enables measurements of the thermal conductivity of rough samples using TDTR. *Published by AIP Publishing.* [http://dx.doi.org/10.1063/1.4952579]

I. INTRODUCTION

Time-domain thermoreflectance (TDTR)[1–3] is a robust pump-probe technique that is widely applied to measure the thermal conductivity of bulk materials[4–6] and nanostructures[7–9] and the thermal conductance of interfaces.[10–14] A schematic diagram of the TDTR setup in our lab is shown in Fig. 1. In a typical TDTR setup, laser pulses from a Ti:sapphire laser are split into pump and probe beams. The pump beam, modulated at a modulation frequency f by an electro-optical modulator (EOM), heats the sample periodically. The temperature response at the sample surface at frequency f is then monitored by the time-delayed probe beam measured by a Si photodiode detector, via change of reflectance with temperature (i.e., thermoreflectance, dR/dT). The value of dR/dT of the transducer metals used in TDTR measurements is, however, usually small, on the order of 10^{-4}–10^{-5} K^{-1}.[15] To measure this small change of intensity of the reflected probe beam, a radio-frequency (RF) lock-in amplifier is employed to pick up signals only at f and reject signals and noises at other frequencies. However, the RF lock-in amplifier does not reject signals from the pump beam that is also modulated at f. Thus, in typical TDTR measurements, special care is given to ensure that the photodetector does not collect any reflected light from the pump beam. For smooth samples, this can be conveniently achieved by blocking the specularly reflected pump beam using an aperture. For rough samples, however, the pump beam is diffusely scattered and thus cannot be blocked by an aperture. Due to the small value of dR/dT ($\sim 10^{-4}$ K^{-1}), the artifact signals, due to the diffusely scattered pump beam that is collected by the photodetector (often called the leaked pump beam), could strongly affect TDTR measurements even if its intensity is <0.01% than that of the reflected probe beam.

Usually, the artifacts due to the leaked pump beam are eliminated via either a two-tint[16] or a two-color approach.[17] In the two-color approach, either the pump or the probe beam is frequency-doubled through second harmonic generation. The leaked pump beam can then be easily rejected using an appropriate optical filter. In the two-tint approach, on the other hand, the pump and probe beams with slightly different wavelengths are created using sharp-edged bandpass and lowpass optical filters.[16] The diffusely scattered pump beam is rejected by placing another sharp-edged filter before the photodetector. Due to less complex instrumentation of the two-tint approach and smaller laser spot sizes that can be achieved, we usually use the two-tint approach to measure rough samples in our lab. One problem for the two-tint approach is that due to sharp edges of the optical filters, fluctuations in the wavelength of the laser often translate into fluctuations in the intensity of the pump and probe beams. Thus, the signal-to-noise ratio (SNR) of two-tint measurements could be significantly reduced from what could be achieved without the

a)Author to whom correspondence should be addressed. Electronic mail: mpekyk@nus.edu.sg

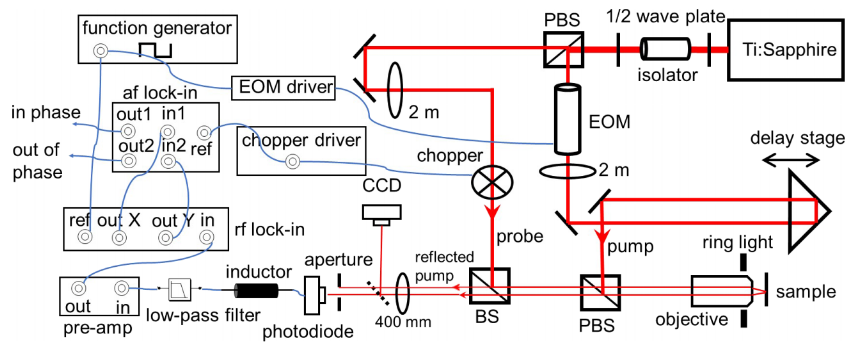

FIG. 1. A schematic diagram of the TDTR setup in our lab. EOM, PBS, and BS represent electro-optic modulator, polarizing beam splitter, and non-polarizing beam splitter, respectively. The convex lenses in the setup are labeled with the respective focal length.

sharp-edged filters, especially when we need to increase the spectral separation of the pump and probe beams to reject a large amount of leaked pump beams as we measure very rough samples.

While the artifact signals due to the leaked pump beam are ubiquitously observed in different labs, the reasons why the artifact signals are even captured during TDTR measurements are still unknown. In a double-modulation TDTR setup (as in our lab), the pump beam is modulated at a radio frequency (e.g., 10 MHz), while the probe beam is modulated at an audio frequency (AF) (e.g., 200 Hz). So, in addition to the RF lock-in amplifier, a second audio frequency (AF) lock-in amplifier is used to eliminate any artifact signals (e.g., coherent pick-ups by the cables) captured by the RF lock-in amplifier. Since the pump beam does not have any audio-frequency components, any artifact signals from the leaked pump beam should be rejected by the second AF lock-in amplifier. Also, it is interesting that the artifact signals due to the leaked pump beam are only observed when the probe beam is not blocked. This shows that the leaked pump beam is modulated at the audio frequency by the probe beam, but it is still unclear at which point in TDTR measurements that the modulation occurs.

In this work, we systemically studied the factors affecting the artifact signals in TDTR measurements due to the leaked pump beam and successfully identified the source of modulation of the leaked pump beam at the audio-frequency of 200 Hz. We find that, when we intentionally increase the leaked pump beam, the in-phase TDTR signal V_{in} is essentially unchanged while the absolute value of out-of-phase TDTR signal V_{out} increases significantly. To better understand the observation, we define a proportionality constant $\alpha = -\Delta V_{out}/\Delta V_{leak}$ to quantify the change of V_{out} in TDTR measurements with the amplitude of the leaked pump beam registered by the RF lock-in amplifier V_{leak}. We find that α only depends on the photocurrent of the photodiode and the Q-factor of the resonate circuit in the TDTR setup. We then experimentally demonstrate that such dependence is due to a slight phase rotation in the phase of the leaked pump beam induced by the reflected probe beam. This phase rotation provides the necessary modulation to the leaked pump beam at the audio frequency of the AF lock-in amplifier. We then developed a simple correction approach to eliminate the artifact signals of the leaked pump beam and thus enable measurements of the thermal conductivity of rough samples using TDTR. We apply this method on a rough InN sample and successfully obtain the correct thermal conductivity for the sample. We show that the pump-leak correction approach could be applied to almost all homogeneously rough samples. We also demonstrate that, for the same level of leaked pump beam, our approach yields much higher signal-to-noise ratio compared to that of the two-tint method and thus establishes the superiority of the new approach.

II. ARTIFACT SIGNALS FROM LEAKED PUMP BEAM

Fig. 1 shows a schematic diagram of the TDTR setup in our lab. Here, we focus on discussing the signal processing in TDTR and readers are referred to Ref. 18 for detailed descriptions on how we acquire and analyze TDTR measurements. Our laser is a femtosecond Ti:sapphire ultrafast laser with a repetition rate of $1/\tau$ = 80 MHz. In the frequency domain, laser pulses from the ultrafast laser are represented by a series of delta functions at multiples of $1/\tau$. We employ a double-modulation approach in our TDTR measurements. In the double-modulation scheme, the pump beam is modulated by an EOM at a radio frequency f_r (e.g., 10 MHz), while the probe beam is modulated by a mechanical chopper at an audio frequency of f_a = 200 Hz. Due to the RF modulation, both the pump beam and the temperature oscillation at the sample surface induced by the pump beam have frequency components of $m/\tau \pm f_r$, where m is an integer. (Here, we do not consider components at higher harmonics of f_r, since they are removed by a RLC resonant circuit, see below.) On the other hand, since the temperature oscillation is monitored by the probe beam via thermoreflectance, the reflected probe beam, measured by a photodiode, is modulated at both the radio frequency f_r and the audio frequency f_a. Thus, the reflected probe beam has frequency components of $m/\tau \pm f_r \pm f_a$. (Again, we do not consider components at higher harmonics of f_a, since they are not picked up by the AF lock-in amplifier, see below.) We use a 30 MHz lowpass filter to remove signals at higher multiples of $1/\tau$ and use a RLC resonant circuit to eliminate the higher harmonics of f_r. (The RLC resonant circuit is formed by serially connecting an inductor to the photodiode, with the photodiode acting as a capacitor.) The RLC resonant circuit also enhances signals around f_r by a factor of Q, the quality factor of the resonant circuit.

Even after the amplification by the RLC resonant circuit and a pre-amp, the signals due to the temperature oscillation are still comparably smaller than the signals at $1/\tau$ and the noise due to the small dR/dT (10^{-4}-10^{-5} K^{-1}) of the metal transducer.[15] Thus, we employ a RF lock-in amplifier to pick up only the minute signals due to the temperature oscillation at sample surface at $\pm f_r \pm f_a$. In the RF lock-in amplifier, we set the time constant to 100 μs, so that the bandwidth of the RF lock-in amplifier (~3 kHz) is sufficiently large to capture the sidebands due to modulation at the audio frequency f_a. However, at this point, artifact signals at f_r will also be picked up by the RF lock-in amplifier. The sources of the artifact signals include, for example, coherent pickups due to RF electromagnetic waves in resonance with the cables and electronic devices in the TDTR setup, and a small amount of pump beam leaked into the photodetector. After demodulation at the radio frequency f_r, the in-phase and out-of-phase outputs of the RF lock-in amplifier, now only with frequency components of $\pm f_a$, are fed into an AF lock-in amplifier. Since the AF lock-in amplifier only pick up the signals with an f_a component, the artifact signals should be rejected by the AF lock-in amplifier as they lack $\pm f_a$ components.

We find that even with the double-modulation approach, the artifact signals from the pump beam leaked into the photodetector are still registered by the AF lock-in amplifier in TDTR measurements. To demonstrate this point, we monitored the in-phase V_{in} and the out-of-phase V_{out} TDTR signals of a 99.99% pure copper coated with a 91-nm-thick Al film, while the pump beam was intentionally and systematically leaked into the photodetector by adjusting the position of the aperture, see Fig. 1. We plot V_{in} and V_{out}, registered by the AF lock-in amplifier, as a function of the signal due to the leaked pump beam V_{leak}, registered by the RF lock-in amplifier, in Fig. 2. We can directly compare V_{in}, V_{out}, and V_{leak}, since they all are amplified by the same factor after being measured by the photodetector. Note that while V_{in} and V_{out} are TDTR signals registered by the AF lock-in amplifier,

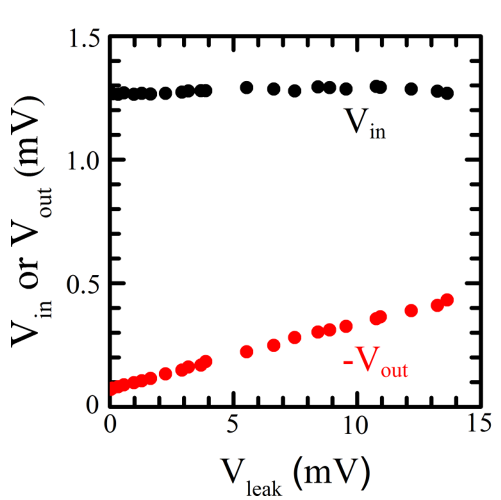

FIG. 2. In-phase (V_{in}) and out-of-phase (V_{out}) TDTR signals as a function of intensity of the leaked pump beam (V_{leak}), measured at delay time of 85 ps with f_r = 10 MHz. The sample is a 99.99% pure Cu substrate, coated with a 91-nm-thick Al. The phase is determined when the leaked pump is minimum and kept unchanged during the measurements. The photocurrent is 0.4 mA and the Q-factor of the RLC resonant circuit is 11.

V_{leak} is not a TDTR signal but is essentially an intensity of the leaked pump beam measured by the photodetector. We set the phase in the reference channel of the RF lock-in amplifier when V_{leak} = 0 and kept the same phase as we increased V_{leak}. We find that as V_{leak} increases, the magnitude of V_{out} increases linearly, see Fig. 2. Interestingly, we find that even when V_{leak} is >10 times larger than V_{in}, V_{in} is still independent of V_{leak}. This trend is not confined to the measurements of the Al/Cu sample that we present in Fig. 2 but generic to all samples we measured. The change of V_{out} due to V_{leak} suggests that the leaked pump beam is modulated at f_a and thus registered by the AF lock-in amplifier.

We postulate that modulation of the leaked pump beam at f_a could occur at either sample surfaces or at the photodetector, since both the pump and the probe beams cross paths at these locations. If the modulation of the pump beam occurs at sample surfaces, properties of the samples (i.e., substrates and the metal transducer) may affect the artifact signals due to the leaked pump beam. On the other hand, if the modulation occurs at the photodetector, properties related to the photodetector such as photocurrent of photodetector and Q-factor of the RLC resonant circuit may affect the artifact signals.

To better pinpoint the origins of the artifact signals of the leaked pump beam, we define a proportionality constant $\alpha = -\Delta V_{out}/\Delta V_{leak}$ to quantify the change of the out-of-phase signal (V_{out}) due to the leaked pump beam. We measured α for 3 samples (Al/Cu, Al/SiO_2, and Cr/SiO_2, where the transducer films are ~90 nm thick) using a wide range of experimental parameters mentioned above. We achieve different photocurrents by changing the intensity of the reflected probe beam and the responsivity of the photodetector (by changing the wavelength of the probe laser). We estimate the photocurrent of the photodetector by measuring the voltage across a 50 Ω resistor serially connected to the photodetector. We modify the Q-factor and the resonant frequency f_r of the RLC circuit by changing the resistor and the inductor in the RLC circuit. We determine the Q-factor of the RLC resonant circuit from the full-width-half-maximum of the resonance by measuring the TDTR signals at frequencies around f_r using the RF lock-in amplifier. In addition, we also removed the RLC resonant circuit and measured α at two modulation frequencies f_r (i.e., 1 MHz and 10 MHz, see the solid symbols in Fig. 3(b)) without the resonant circuit.

We summarize the measured α in Fig. 3, as a function of the photocurrent and Q-factor. We find that the proportionality constant α from the leaked pump beam does not depend on the type of samples and transducers, see Fig. 3(a), suggesting that the modulation of the leaked pump beam at f_a does not occur at the sample surfaces. On the other hand, we find that α depends strongly on the properties related to the photodetector, i.e., photocurrents in the photodetector and Q-factor of the RLC circuits. The dependences on both the photocurrent and the Q-factor are linear, see Fig. 3. Since both factors are affected by the photodetector, Fig. 3 suggests that the modulation of the signals from the leaked pump beam at f_a occurs at the photodetector. Interestingly, we also find that α is small but nonzero after we remove the RLC resonant circuit, see Fig. 3(a).

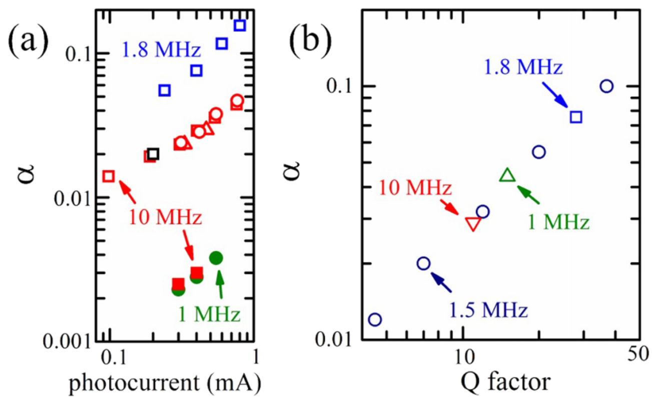

FIG. 3. (a) The proportionality constant α as a function of photocurrent in the photodetector, measured on Al/Cu (squares), Al/SiO_2 (circles), and Cr/SiO_2 (triangles). The measurements were performed using a laser wavelength of 787 nm (red, blue, olive) and 850 nm (black), at a modulation frequency f_r of 10 MHz (red and black), 1.8 MHz (blue), and 1.0 MHz (olive), with (open symbols) and without (solid symbols) the RLC resonant circuit. The symbols are labeled with the modulation frequency f_r used in the TDTR measurements. (b) The proportionality constant α as a function of the Q-factor of the RLC resonant circuit. The measurements were performed using a laser wavelength of 787 nm, a photocurrent of 0.4 mA, and at a modulation frequency as labeled. Different Q-factors are achieved by changing the resistance and the inductance of the RLC circuit.

One possible explanation to the observed modulation of the leaked pump beam at the photodetector is that the probe beam prompts a phase rotation in the V_{leak} measured by the photodetector. To demonstrate this point, we consider the photodetector being simultaneously illuminated by the probe beam modulated by a 50% duty cycle "on-off" square wave at f_a and the leaked pump beam. During the "off"-state, the leaked pump beam is fully synchronized with the reference signals of the RF lock-in amplifier; thus, V_{leak} is registered as in-phase signal in the RF lock-in amplifier. During the "on"-state, however, illumination of the probe beam could induce a small phase rotation of Δθ to the phase of the leaked pump beam. Due to the phase rotation, the in-phase and out-of-phase signals of the leaked pump beam registered by the RF lock-in amplifier are rotated by ΔV^{in}_{leak} and ΔV^{out}_{leak}, respectively. Thus, the outputs of the RF lock-in amplifier due to the leaked pump beam during both the "on" and "off" states constitute a square wave of frequency f_a, with amplitudes of ΔV^{in}_{leak} and ΔV^{out}_{leak}, respectively. These signals at f_a are then captured by the AF lock-in amplifier. As long as Δθ is sufficiently small, ΔV^{in}_{leak} and ΔV^{out}_{leak} can be approximated as

$$\begin{aligned} \Delta V^{in}_{leak} &= 0, \\ \Delta V^{out}_{leak} &= -V_{leak} \times \Delta\theta, \end{aligned} \tag{1}$$

where the minus sign accounts for the 180° out-of-phase of the outputs of the RF lock-in amplifier due to the leaked pump beam and the reference signals of the AF lock-in amplifier. The expected results of Eq. (1) are consistent with our observation that the leaked pump beam only affects the out-of-phase TDTR signals, not in-phase, see Fig. 2.

To verify that the artifact signals are due to the phase rotation in the photodetector, we experimentally measure Δθ using two different approaches and compare the measurements to α derived from our TDTR measurements with increasing leaked pump beam intensity. In the first approach, we purposely separate the pump and probe beams at sample surfaces by ∼25 μm and perform TDTR measurements with a controlled amount of pump beam leaked into the photodetector. As the pump and probe beams do not overlap, TDTR signals (i.e., V_{in} and V_{out}) are zero. Thus, we can directly measure ΔV^{in}_{leak} and ΔV^{out}_{leak} from the outputs of AF lock-in amplifier. As expected, $\Delta V^{in}_{leak} \approx 0$ as suggested by Eq. (1). We then calculate Δθ from ΔV^{out}_{leak} and V_{leak}, using Eq. (1). In the second approach, we directly measured the phases of the leaked pump beam in the RF lock-in amplifier, with and without illumination of the probe beam, and derived Δθ from the difference in the measured phases. The phase of the leaked pump beam is readily determined from the phase of the reference channel of the RF lock-in amplifier when the out-of-phase channel is zero. The uncertainty of Δθ is estimated from the standard deviation of the outputs of the RF lock-in amplifier. We compare Δθ derived using both approaches to α measured at the same photocurrent and Q in Fig. 4. We note that Δθ derived using the second approach is ∼10% higher than Δθ derived using the first approach, see Fig. 4. This small difference could be due to, e.g., imperfect modulation of the leaked pump beam as a result of a finite rise time of the photodetector. We confirm that Δθ = α within experimental uncertainty for Δθ derived using both approaches, see Fig. 4.

We are not certain of the sources of the phase rotation. One possible reason is that the junction capacitance of the p-i-n photodiode is slightly changed while illuminating and thus alters the resonance of the RLC circuit. However, this cannot explain why we still observe the phase rotation even without the RLC resonant circuit.

III. TDTR MEASUREMENTS OF ROUGH SAMPLES

We can easily correct the artifact signals due to leaked pump beam using Eq. (1) and thus enable TDTR

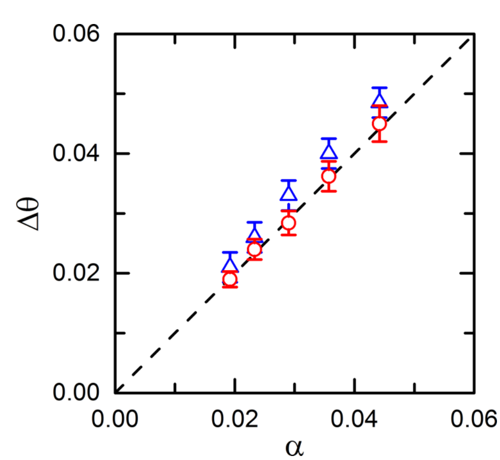

FIG. 4. Comparison of Δθ derived using the first (red circles) and the second (blue triangles) approaches (see the main text for the details of how Δθ was derived), and α derived from TDTR measurements with increasing intensity of the leaked pump as shown in Fig. 2. Measurements were performed on the Al/Cu sample with a modulation frequency of 10 MHz (Q = 11), with V_{leak} of 1 mV. The photocurrents are 0.19 mA, 0.31 mA, 0.40 mA, 0.54 mA, and 0.76 mA, respectively.

measurements on rough samples. To achieve the pump-leak correction, we simultaneously monitor the intensity of the leaked pump beam V_{leak} registered by the RF lock-in amplifier, while we perform TDTR measurements. In our setup, this can be readily achieved by monitoring the offsets of the square wave inputs to the AF lock-in amplifier, in addition to the amplitudes of the square waves usually monitored during typical TDTR measurements; V_{leak} equals the offset of the input to the in-phase channel. To ensure a sufficiently high signal-to-noise (>50) for the V_{leak} measured by this approach, we set the time constant of the AF lock-in amplifier to 700 ms. We assume a linear system and superposition of TDTR signals and the artificial signals due to the leaked pump beam. Thus, we can correct our original TDTR signals by subtracting the ΔV_{leak}^{out} calculated using Eq. (1) from V_{out}.

In conventional TDTR, the phase of the reference channel of RF lock-in amplifier is determined by the fact that the out-of-phase signal V_{out} is constant when the delay time crosses t = 0.[1] When there is a leaked pump beam, V_{out} is composed of the "real" out-of-phase TDTR signal and artificial signal ΔV_{leak}^{out} from the leaked pump beam. As we mentioned in Sec. II, ΔV_{leak}^{out} is independent of delay time. Thus, we can still use the same way as conventional TDTR to determine the phase when there is a leaked pump beam and applying our pump-leak correction approach to measure rough samples.

We test our pump-leak correction approach on an Al/InN/GaN/sapphire sample. The InN film is 2.5 μm thick and was deposited by a molecular beam epitaxy (MBE), provided to us by Prof. Gregor Koblmueller of Technical University of Munich (TUM).[19] The sample is rough because a high lattice constant mismatch between InN and the substrate produces a high concentration of line defects in the InN film and a rough surface morphology. We coated the InN sample with ~98 nm thick Al by thermal evaporation. The thickness of Al is determined by picosecond acoustics[20,21] as in conventional TDTR, since the in-phase signal V_{in} is hardly affected by the leaked pump beam. To validate our new approach, we performed conventional TDTR, two-tint TDTR, and TDTR with the pump-leak correction on the rough InN sample. In all the TDTR measurements, we used laser $1/e^2$ radii of 4.5 μm, a modulation frequency f_r of 10 MHz for the pump beam, and an audio-frequency f_a of 200 Hz for the probe beam. We employed a total laser power of 60 mW to ensure that the temperature rise on the sample is <5 K. We used appropriate natural density filters before the photodetector to fix the photocurrent of the photodetector at ~0.4 mA.

We performed TDTR measurements at two spots (Spots A and B) on the rough InN sample. Spot A (Fig. 5(a)) is relatively smooth with 96% of light incident on the spot being specularly

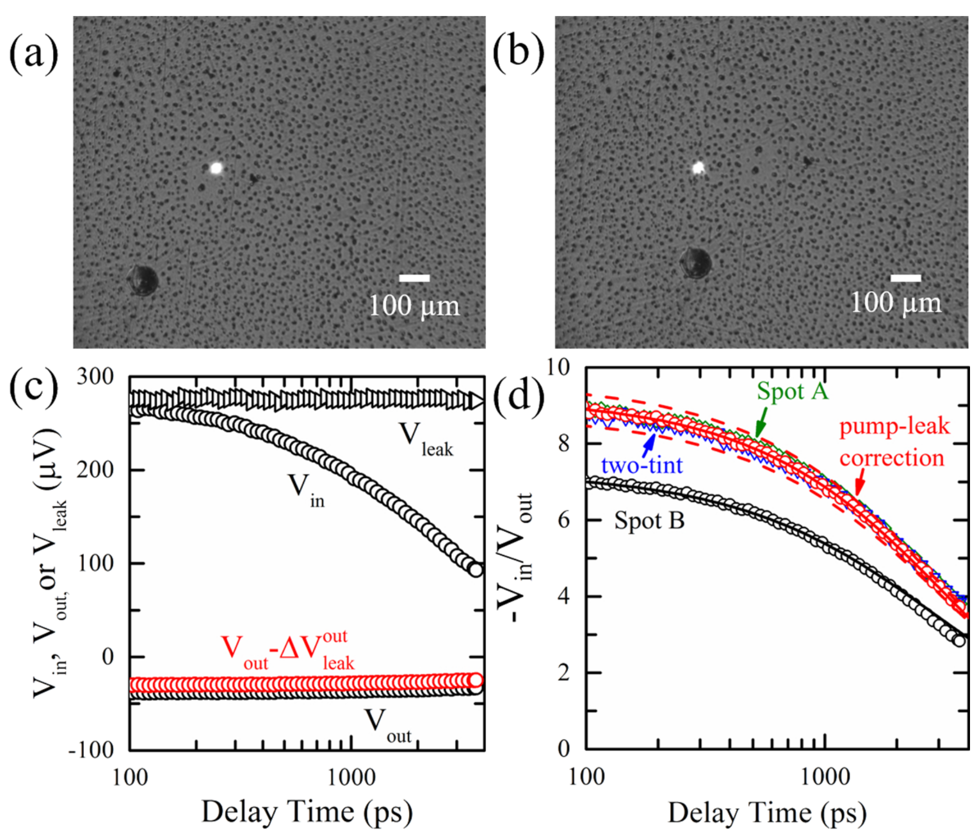

FIG. 5. Bright-field microscope images of an Al/InN/GaN/sapphire sample when TDTR measurements were performed at (a) relatively smooth Spot A and (b) rough Spot B. The white dots in the images are the laser spots. (c) V_{in}, V_{out}, and V_{leak} measured at Spot B (black), as labeled. V_{out} is instantaneously corrected using ΔV_{leak}^{out} calculated from Eq. (1) (red) in our pump-leak correction approach. (d) Conventional TDTR measurements at Spot A (olive diamonds, labeled "Spot A") and Spot B (black circles, labeled "Spot B"), compared to measurements at Spot B using the pump-leak correction approach (red circles, labeled "pump-leak correction") and the two-tint approach (blue triangles, labeled "two-tint"). Solid lines are calculations using a thermal model assuming $\Lambda = 98$ W m^{-1} K^{-1} (red) and $\Lambda = 62$ W m^{-1} K^{-1} (black), respectively, while the dashed lines are calculations with the Λ varied by ±10%. For all the measurements, we use a modulation frequency of 10 MHz (Q = 11), a spot size of 4.5 μm, a total power of 60 mW, and a photocurrent of 0.4 mA.

reflected. We find that $V_{leak} < 0.3V_{out}$ at this spot, implying that ΔV^{out}_{leak} is less than 1% of V_{out}. We derive the thermal conductivity of InN, $\Lambda = 98$ W m^{-1} K^{-1}, from conventional TDTR measurements at Spot A, see the olive diamonds in Fig. 5(d). The result is in good agreement with our previous measurement on a 1-μm-thick InN film[22] and is ∼20% smaller than the measured thermal conductivity of 0.5-2.1 μm thick InN films.[23] Spot B (Fig. 5(b)), on the other hand, is rough, with only 80% of light incident on the spot being specularly reflected. At this spot, $V_{leak} > 6V_{out}$, see Fig. 5(c). Due to the high level of leaked pump beam, conventional TDTR measurement yields a wrong result of only 62 W m^{-1} K^{-1}, see the black circles in Fig. 5(d). We thus applied the pump-leak correction approach that we developed to derive the thermal conductivity at this spot. We simultaneously measured V_{leak}, V_{in}, and V_{out} for every delay time, see Fig. 5(c). We note that V_{leak} is stable in delay time with a standard deviation of only ∼2.5%, indicating that a time constant of 700 ms is sufficient for the AF lock-in amplifier. We calculated ΔV^{out}_{leak} from V_{leak} using Eq. (1) and $\Delta\theta = 0.029$ for photocurrent of 0.4 mA derived from Fig. 3(a). We corrected V_{out} using the derived ΔV^{out}_{leak}, see the red circles in Figs. 5(c) and 5(d). Excellent agreement is achieved between the TDTR measurements at Spot B after the pump-leak correction and the conventional TDTR measurements at Spot A with a smooth surface, see Fig. 5(d).

We also employed the two-tint approach to reject the leaked pump beam in TDTR measurements at Spot B, see the blue triangles in Fig. 5(d). Excellent agreement is achieved, suggesting that both the two-tint and the proposed pump-leak correction approaches could be applied in TDTR measurements of rough samples. We note, however, that the signal-to-noise ratio of our two-tint measurements is only ∼32, a factor of three smaller than our measurements using the pump-leak correction approach. The reason for this small signal-to-noise ratio is that, in the implementation of the two-tint approach, we need to increase the separation between the wavelengths of the pump and the probe beams to enhance the suppression of the high level of leaked pump beam. As a result, fluctuations in the wavelength of the laser are more significantly translated into fluctuations in the intensity of the laser beams, leading to higher noise.

IV. LIMITS OF THE PUMP-LEAK CORRECTION APPROACH

Here, we establish a limit for the pump-leak correction approach and compare our new approach to the two-tint method. To achieve this purpose, we performed a series of TDTR measurements on a bulk single-crystalline Cu sample coated with a 100-nm-thick Al film, with different levels of pump beam leaked into the photodiode, to mimic TDTR measurements on samples with different roughnesses. We choose the Al/Cu sample because the ratios $-V_{in}/V_{out}$ in TDTR measurements of the sample are high, and thus, TDTR measurements are more susceptible to the artifacts due to leaked pump beam. We intentionally removed the aperture in the TDTR setup and systematically changed the distance between the pump and probe beams to achieve different levels

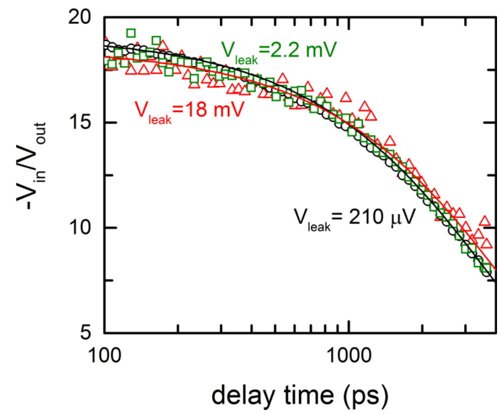

FIG. 6. TDTR measurements of Al/Cu sample after the pump-leak correction approach. The initial leaked pump levels before the correction are $V_{leak} = 210$ μV (black solid spheres), 2.2 mV (olive open squares), and 18 mV (red solid spheres), respectively. The solid lines are fits to the TDTR measurements after pump-leak correction. For all our measurements, we set the probe power at 5 mW, the pump power at 120 mW, $f = 10$ MHz, the laser spot size at 5 μm, and the photocurrent of the photodiode at ∼0.45 mA and use $\alpha = 0.033$ for the pump-leak correction.

of pump leak. We quantify the leaked pump beam using the ratio $V_{leak}/|V_{out}|$, where V_{leak} and V_{out} are defined as before. For the pump power of 120 mW, the probe power of 5 mW, a spotsize of 5 μm, and a modulation frequency of 10 MHz, we achieved V_{leak} ranging from 40 μV to 18 mV, $|V_{out}|$ was fixed at 150 μV, and thus $V_{leak}/|V_{out}|$ ranging from 0.26 to 120.

We then applied the pump-leak correction approach to the TDTR measurements acquired on the Al/Cu sample, see Fig. 6, using $\alpha = 0.033$ derived from Fig. 3(a). We find that for the case of $V_{leak} = 18$ mV, the measurements are still slightly affected by the leaked pump beam, even after the pump-leak correction. Nevertheless, we derived the thermal conductivities of Cu and found that the values are still within the range of 400 W m^{-1} K^{-1} ± 5%. This value of the thermal conductivity of Cu is in good agreement with the literature value.[24]

To set a limit on the applicability of the pump-leak correction approach, we consider a safe case of $V_{leak}/|V_{out}| = 15$ ($V_{leak} = 2.2$ mV in Fig. 6). Taking into consideration the solid angle of the aperture and the reduced TDTR signals by the rough samples, we estimate that $V_{leak}/|V_{out}| = 15$ is achieved when TDTR measurements are performed on rough samples with only ∼1% of the light being specularly reflected. Thus, the proposed pump-leak correction approach could be used for measurements of practically all rough samples, as long as the roughness is homogeneous. For inhomogeneously rough samples, however, laser beams are distorted at sample surfaces and thus the assumption of a Gaussian distribution of laser beams in the thermal model is violated. As a result, analysis of TDTR measurements does not yield correct results, even though the pump-leak correction approach successfully removes the artifacts due to leaked pump beam.

We summarize signal-to-noise ratios (SNR) of TDTR measurements ($-V_{in}/V_{out}$ at 100 ps) of the Al/Cu sample after the pump-leak correction approach in Fig. 7. We find that while SNR drops when $V_{leak}/|V_{out}|$ increases, a decent SNR of ∼40 is still achieved when $V_{leak}/|V_{out}| = 30$, see

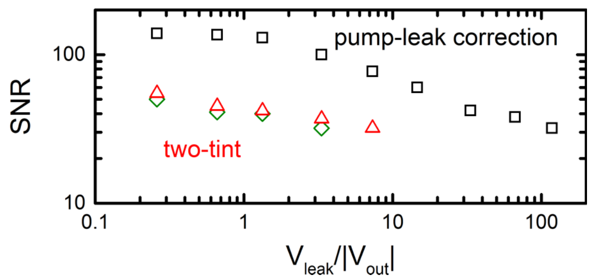

FIG. 7. Signal-to-noise ratios (SNR) of TDTR measurements on an Al/Cu sample using the pump-leak correction approach (black square) and the two-tint approach (red triangles and olive diamonds). In the implementation of the two-tint approach, we tilt the long-pass filter in the route of the pump beam such that the pump power after long-pass filter is reduced to 40% (red triangles) and 20% (olive diamonds) of the original power, respectively. We then eliminate the artifact signals from the leaked pump beam using a second bandpass filter before the photodiode. All other experimental parameters are as in Fig. 6.

Fig. 7. For comparison, we also plot the SNR of TDTR measurements acquired using the two-tint approach. We find that using our setup, the SNR for the pump-leak correction approach is a factor of ~2 better, compared to that of the two-tint approach. The reason for the poor SNR for the two-tint approach (compared to, e.g., that reported in Ref. 16) is that our laser (from the Coherent Chameleon family), like many other ultrafast lasers, is fully automated to optimize stability in laser intensity but not in laser wavelength. As a result, fluctuations in laser wavelength are translated into fluctuations in the pump and probe powers and appear as noise in TDTR measurements.

V. CONCLUSION

In conclusion, we developed a pump-leak correction approach to eliminate the artifact signals due to the leaked pump beam in TDTR measurements of rough samples. We find that the artifact signals originate from a small phase rotation in the signals by the leaked pump beam induced by concurrent illumination of the photodetector by the modulated probe beam. The phase rotation generates an artifact signal in the out-of-phase of TDTR measurements, which can be readily reversed as long as the intensity of the leaked pump beam is monitored during TDTR measurements. Since the intensity of the leaked pump beam can be readily monitored by the AF lock-in amplifier in a typical TDTR setup, our approach does not require any additional optical elements or modification of existing TDTR setup. Also, high signal-to-noise ratios could be readily achieved even when the level of leaked pump beam is high. Our approach thus provides a convenient alternative for TDTR measurements of homogeneously rough samples.

ACKNOWLEDGMENTS

This research is supported by NUS Start-up Grant. We are very grateful to Georg Haunschild and Professor Gregor Koblmueller at Technische Universität München for providing us the InN sample and Yumeng Yang at the ECE department of National University of Singapore for the deposition of Cr.

[1] D. G. Cahill, Rev. Sci. Instrum. **75**, 5119 (2004).
[2] A. J. Schmidt, X. Y. Chen, and G. Chen, Rev. Sci. Instrum. **79**, 114902 (2008).
[3] Y. K. Koh, S. L. Singer, W. Kim, J. M. O. Zide, H. Lu, D. G. Cahill, A. Majumdar, and A. C. Gossard, J. Appl. Phys. **105**, 054303 (2009).
[4] C. Chiritescu, D. G. Cahill, N. Nguyen, D. Johnson, A. Bodapati, P. Keblinski, and P. Zschack, Science **315**, 351 (2007).
[5] X. Zheng, D. G. Cahill, P. Krasnochtchekov, R. S. Averback, and J. C. Zhao, Acta Mater. **55**, 5177 (2007).
[6] Z. Guo, A. Verma, X. Wu, F. Sun, A. Hickman, T. Masui, A. Kuramata, M. Higashiwaki, D. Jena, and T. Luo, Appl. Phys. Lett. **106**, 111909 (2015).
[7] J. Liu, B. Yoon, E. Kuhlmann, M. Tian, J. Zhu, S. M. George, Y. Lee, and R. Yang, Nano Lett. **13**, 5594 (2013).
[8] A. I. Persson, Y. K. Koh, D. G. Cahill, L. Samuelson, and H. Linke, Nano Lett. **9**, 4484 (2009).
[9] B. Saha, Y. R. Koh, J. Comparan, S. Sadasivam, J. L. Schroeder, M. Garbrecht, A. Mohammed, J. Birch, T. Fisher, A. Shakouri, and T. D. Sands, Phys. Rev. B **93**, 045311 (2016).
[10] E. Ziade, J. Yang, G. Brummer, D. Nothern, T. Moustakas, and A. J. Schmidt, Appl. Phys. Lett. **107**, 091605 (2015).
[11] P. E. Hopkins, M. Baraket, E. V. Barnat, T. E. Beechem, S. P. Kearney, J. C. Duda, J. Robinson, and S. Walton, Nano Lett. **12**, 590 (2012).
[12] Y. K. Koh, M. H. Bae, D. G. Cahill, and E. Pop, Nano Lett. **10**, 4363 (2010).
[13] M. D. Losego, M. E. Grady, N. R. Sottos, D. G. Cahill, and P. V. Braun, Nat. Mater. **11**, 502 (2012).
[14] B. Huang and Y. K. Koh, Carbon **105**, 268 (2016).
[15] Y. X. Wang, J. Y. Park, Y. K. Koh, and D. G. Cahill, J. Appl. Phys. **108**, 043507 (2010).
[16] K. Kang, Y. K. Koh, C. Chiritescu, X. Zheng, and D. G. Cahill, Rev. Sci. Instrum. **79**, 114901 (2008).
[17] A. Schmidt, M. Chiesa, X. Y. Chen, and G. Chen, Rev. Sci. Instrum. **79**, 064902 (2008).
[18] P. Jiang, B. Huang, and Y. K. Koh, e-print arXiv:1511.04852 (2015).
[19] C. S. Gallinat, G. Koblmüller, F. Wu, and J. S. Speck, J. Appl. Phys. **107**, 053517 (2010).
[20] C. Thomsen, H. T. Grahn, H. J. Maris, and J. Tauc, Phys. Rev. B **34**, 4129 (1986).
[21] W. P. Hsieh and D. G. Cahill, J. Appl. Phys. **109**, 113520 (2011).
[22] J. Ju, B. Sun, G. Haunschild, B. Loitsch, B. Stoib, M. S. Brandt, M. Stutzmann, Y. K. Koh, and G. Koblmüller, AIP Adv. **6**, 045216 (2016).
[23] A. X. Levander, T. Tong, K. M. Yu, J. Suh, D. Fu, R. Zhang, H. Lu, W. J. Schaff, O. Dubon, W. Walukiewicz, D. G. Cahill, and J. Wu, Appl. Phys. Lett. **98**, 012108 (2011).
[24] R. W. Powell, C. Y. Ho, and P. E. Liley, "Thermal conductivity of selected materials," U.S. Department of Commerce, National Bureau of Standards, 1966.